Green Chemistry

PAPER

View Article Online
View Journal | View Issue

Cite this: *Green Chem.*, 2025, **27**, 15654

La-based perovskite structures as efficient heterogeneous catalysts for acceptorless dehydrogenative coupling of alcohols and amidines toward pyrimidines

Sándor Balázs Nagy,†[a] Anna Adél Ádám,†[a] Bence Kutus,[a] Gergely Ferenc Samu,[a,b] Ákos Kukovecz,[c] Zoltán Kónya[c,d] and Gábor Varga*[c]

Received 18th September 2025,
Accepted 15th November 2025

DOI: 10.1039/d5gc04945h

rsc.li/greenchem

The synthesis of fine chemicals using biomass-derived reagents has already emerged as one of the most urgent challenges, for which, many alternative green approaches to the well-known organic transformations need to be developed. In line with this concept, a novel green process for the heterogeneous catalytic acceptorless dehydrogenative coupling (ADC) of benzamidine and biomass-derived alcohols to pyrimidines is presented in this work. In contrast to the well-established heterogeneous Pt/C catalysis (EcoScale of 64) operating under harsh reaction conditions, we are able to build a green process (EcoScale of 81) based on the use of $LaCoO_3$ perovskite catalyst allowing an exclusively selective (84% isolated yield of pyrimidine) cyclization at ~80 °C within only 8 hours even in a green solvent (2-Me-THF). In addition, the structure–activity relationship of this catalyst was also successfully uncovered, showing a cooperatively acting catalyst. In particular, the La(III)–O^{2-} sites can govern the activity of the catalyst, while the Co(III)–O^{2-} centers dictate the selectivity of the perovskite. Furthermore, the $LaCoO_3$ structure proved to be a recyclable and highly substrate-tolerant promoter, which is essential for producing substituted pyrimidines.

Green foundation

1. In this manuscript, we present the first sustainable and heterogeneous catalytic process for the production of pyrimidines, which are of great importance in many different industrial processes, by replacing homogeneous palladium catalysts with $LaCoO_3$ perovskite.
2. The $LaCoO_3$ perovskite oxide proved to be a very efficient (up to 93 mol% conversion), versatile and selective (up to 100 mol% substituted pyrimidine selectivity) catalyst which enables a three component acceptorless dehydrogenative coupling (ADC) process with excellent recyclability (up to 9 runs) and possible regenerability in a green solvent (2-Me-THF) in a ligand-, additive and precious metal-free manner without using inert atmosphere.
3. Since we have determined the structure–activity relationships of this cooperatively operating bifunctional Lewis acid/Co(III) redox-active catalyst, our work can provide important information for the design and development of more sustainable heterogeneous catalytic processes for the production of pyrimidines and other important organic compounds *via* ADC.

1. Introduction

The pyrimidine scaffold is of great importance as a building block for many different heteroaromatic compounds. Many of these use in the pharmaceutical and advanced electronic industries such as antibacterial,[1,2] antiviral,[3] and anticancer drugs,[4,5] push–pull molecules,[6] light emitting materials[7] and non-linear optical elements,[8] reflecting the unique role of pyrimidine compounds.

Although there are many chemical strategies (inverse Diels–Alder reaction, Bredereck protocol, trifluoromethanesulfonic anhydride-mediated cyclization of amides, *etc.*)[9,10] to efficien-

[a]*Department of Molecular and Analytical Chemistry, University of Szeged, Dóm square 7–8, Szeged, H-6721 Hungary*
[b]*ELI ALPS, ELI-HU Non-Profit Ltd., Wolfgang Sandner street 3., Szeged, H-6728 Hungary*
[c]*Department of Applied and Environmental Chemistry and Interdisciplinary Excellence Centre, University of Szeged, Rerrich Béla tér 1, Szeged, H-6720, Hungary. E-mail: gabor.varga5@chem.u-szeged.hu*
[d]*HUN-REN-SZTE Reaction Kinetics and Surface Chemistry Research Group, Rerrich Béla tér 1, H-6720 Szeged, Hungary*
†These authors contributed equally.

tly build this scaffold, these strategies rely on the use of harsh oxidants, expensive and sensitive precursors and noble metal catalysts. In addition, each of the reactants used is of petrochemical origin, and their conversion results in a significant amount of waste.[11–13] Over the last decade, this has motivated researchers to develop new synthetic processes that enable the production of pyrimidine derivatives based on readily accessible, sustainable raw materials.

One of the most powerful developed strategies is the acceptorless dehydrogenative coupling (ADC) pioneered by Kirchner,[14] Kempe[15] and Milstein,[16] which enables an oxidant-free, economically viable, atom-economic reaction of alcohols from indigestible lignocellulosic biomass with amidines to form pyrimidine. This reaction proceeds *via* a multistep sequence that includes the dehydrogenation of the corresponding alcohols as a rate-determining step and selective C–C/C–N condensations.[17,18] Moreover, this process proved to be so versatile that it can also be used for the production of other industrially relevant components such as imines and pyrroles, *etc*. Despite all the listed advantages over the conventional syntheses, ADCs have so far been underutilized both in industry and academia because they require harsh reaction conditions (T = 140–160 °C), an inert atmosphere, non-green solvents (toluene, amino alcohols) and consume a lot of energy since they proceed over a long reaction time of even 24 hours.[19,20] In addition, the whole process generates inorganic waste, especially inorganic bases whose neutralization is a challenge in a safety manner. In addition, it has been considered a privileged area of homogeneous noble metal catalysts (Pt, Pd, Ru, Ir, *etc*.) with the ability to liberate hydrogen from alcohols and be selective in condensations. Among these catalysts, precious metal complexes with pincer-type cooperative ligands have proven to be the most efficient structures.

To replace these efficient but (1) scarce and therefore expensive and (2) less stable precious metals under the reaction conditions of the biomass refinery, which are very different from those of the petroleum refinery, Kempe,[21] Milstein,[22] Kirchner,[23] Balaraman[24] and recently Rengan[25] and others[26–28] have presented new strategies that use redox-active transition metal (TM) ions as catalysts, including Ni, Mn and Co-containing systems that take advantage of pincer complexes containing various – sometimes exotic (*e.g.*, Mn(I) and Co(I)) – oxidation states of the TMs. Although remarkable progress has been made with these complexes, especially in lowering the required reaction temperature (T = 110–130 °C) or stabilizing the structure of the actual catalysts in the reaction mixture, even these processes could not cope with most of the harsh reaction conditions described above, which need to be modified to achieve a sustainable reaction pathway. In addition, no one has yet developed a heterogeneous catalyst for ADC based on pincer complexes, possibly due to their well-tuned/non-flexible structures. It should be noted that ADCs have already been realized heterogeneously, but exclusively over supported noble metal catalysts.[29] For pyrimidine synthesis, the Pt/C catalyst seems to be the best and so far the only efficient choice, but with the same drawbacks that make all the listed processes less suitable.[30]

Nevertheless, computational studies focusing on heterogeneous catalysts for ADCs have shown the need for a well-established, intimate enough interaction between metals and supports to have a chance of producing sufficiently competitive heterogeneous catalysts based on transition metals.[29,31] We also found that a properly created interface between redox-active transition metal ions (Co(II)) and support with Lewis acidic character ($Bi_2O_2CO_3$) can function cooperatively, even enabling ADC reactions.[32] Moreover, to promote the eventual dehydrogenation of alcohols, the supports must have both medium (Lewis) basic and medium (Lewis) acidic sites that can mimic the cooperative effect of the ligand in pincer complexes. Recently, we have shown that La-based perovskite oxides can facilitate multistep reactions in which these oxides play the role of a cooperatively operating, multifunctional catalyst. La_xO_y units provide the Lewis acidic/basic character and Ni centers act as redox-active sites.[33] Many other studies have also shown that perovskites can function heterogeneously in a recyclable manner under mild reaction conditions.[34] In light of these findings, we hypothesized that these La-based structures can meet the requirements to be efficient catalysts for pyrimidine synthesis following an ADC strategy.

In this article, we show that CoLa-containing perovskites and Mn- and Ni-containing ones to some extents are able to allow the synthesis of pyrimidines *via* a heterogeneous catalytic ADC route under considerably mild reaction conditions. A clear relationship between the acidity of the oxide framework and the catalytic performance of the perovskite is presented. Moreover, we were able to prove the cooperative catalytic character of the acidic and redox-active centers co-existing on the surface of the perovskites.

2. Results and discussion

2.1. Proof of concept

According to a well-established sol–gel synthesis method, phase-pure, highly crystalline mixed metal oxides with a perovskite structure were produced. This was clearly demonstrated by XRD patterns (Fig. 1A, Fig. S1A and B) of the as-prepared structures consisting only of the fingerprint-like diffractions (100, 110, 111, 200, 210, 211, 220),[35] which match those of La- and various transition metal-containing perovskites. No other patterns possibly belonging to impurities appeared in the diffractograms, indicating in each case the formation of a single-phase product. Based on the Scherrer equation, the average primary crystallite size for each oxide was between 25–46 nm (Table S1). Similar results were obtained for the layered Ruddlesden–Popper (RP; Fig. 1B, Fig. S1A and B) phase counterparts of the corresponding simple perovskites.[36]

The Raman spectra of the solids also closely resemble those from previous studies.[37] All spectra of the perovskites (Fig. 1C, Fig. S2A and B) contain the characteristic Raman shifts of a series of A_g vibration modes in the 680–500 cm^{-1} range, demonstrating the rhombohedral crystal structure of these oxides. In contrast, the spectra of the RP counterparts (Fig. 1D, Fig. S2B)

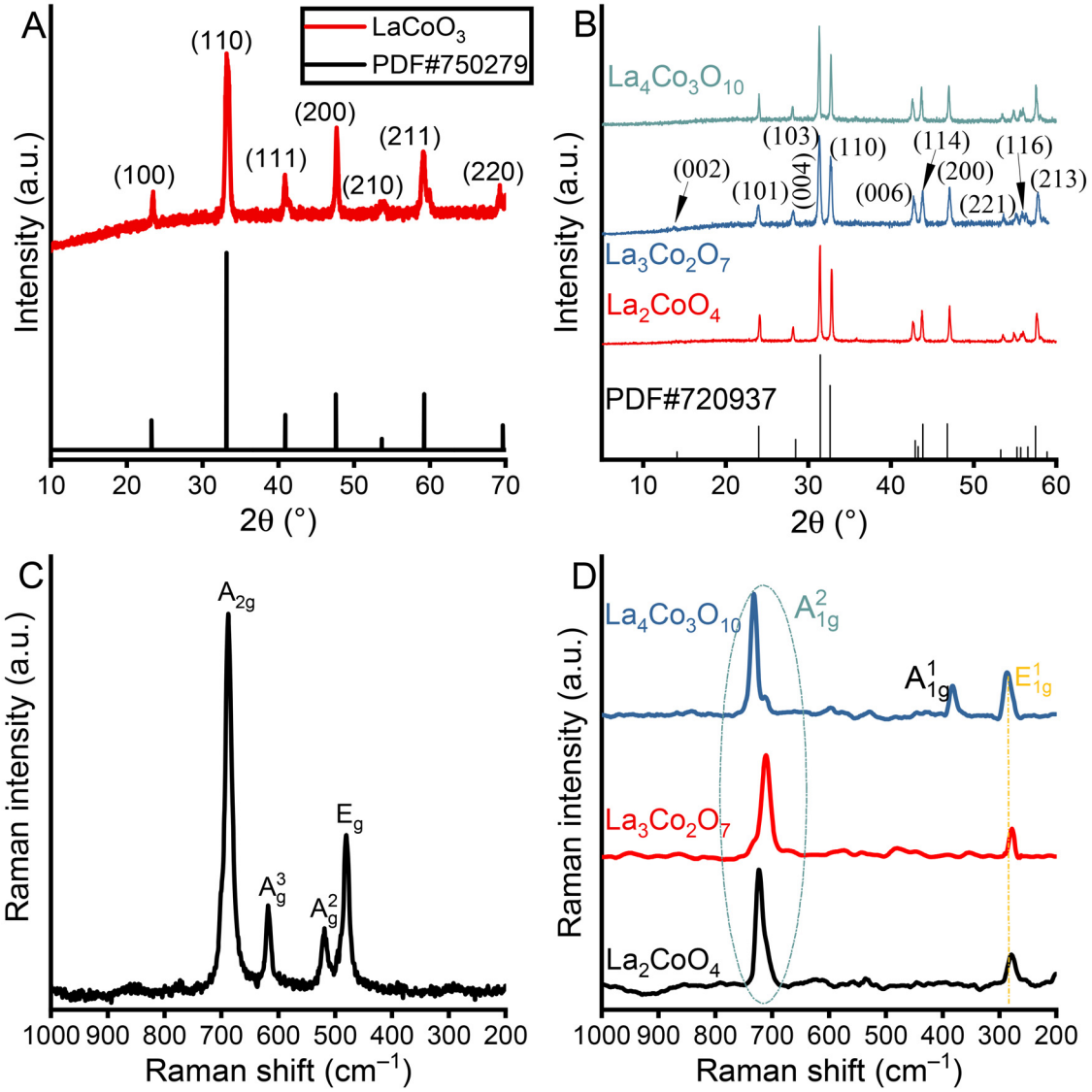

Fig. 1 XRD patterns of LaCo-containing perovskite (A) and RP-phase (B) oxides. Raman spectra of $LaCoO_3$ perovskite (C) and its RP-phase counterparts (D).

exhibit intense peaks in a wider energy range (700–200 cm^{-1}), which are associated with vibration modes of a tetragonal crystal structure.[38] Thus, the peak of the A_{1g} vibration mode dominates the spectra, supporting the existence of the tetragonal structure. Furthermore, there is no evidence for the (co-)existence of anionic specimens or other Raman-active components as impurities (carbonates, nitrates, *etc.*) in the as-prepared structures. Besides, the ICP-MS measurements (Table S1) confirmed the equality of the theoretical and the actual M/La ratios (M: Cu, Ni, Mn, Co) in the bulk within the margin of error of the method in all cases. Consequently, catalytic tests (Scheme 1) investigate the performance of monophasic perovskite oxides and their layered counterparts in the absence of any impurities.

With these oxide structures in hand and using the reaction conditions that proven to be generally useful for ADCs,[30] an attempt was made to determine whether the perovskites are capable of promoting this transformation. Accordingly, ADC test reactions (Scheme 1) of phenyl ethanol, benzyl alcohol and benzamidine hydrochloride were carried out in equimolar ratios (0.25 mmol) in toluene (2 mL) in the presence of the corresponding oxides of 10 mol% and an inorganic base (^{t}BuOK of 0.50 mmol) for 24 h at reflux under a N_2 atmosphere. As can be seen in Fig. 2, no reaction occurred in the absence of any catalyst, whereas when the heterogeneous ADC was repeated using a commercially available Pt/C catalyst, a high conversion of the benzamidine (92%) to the pyrimidine product (100% product selectivity) was achieved, which is in good agreement with the literature data.[30] In comparison, each perovskite structure (Fig. 2, Fig. S3) enables this conversion to some extent, with pure to moderate benzyl alcohol conversions (39–54 mol%) being achieved with reasonable pyrimidine selectivity (55–65 mol%). This clearly reflects the main-

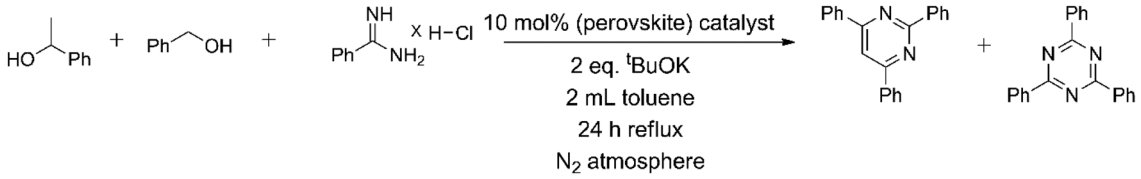

Scheme 1 Heterogeneously catalyzed ADC test reaction: pyrimidine and triazine synthesis from alcohols and amidines.

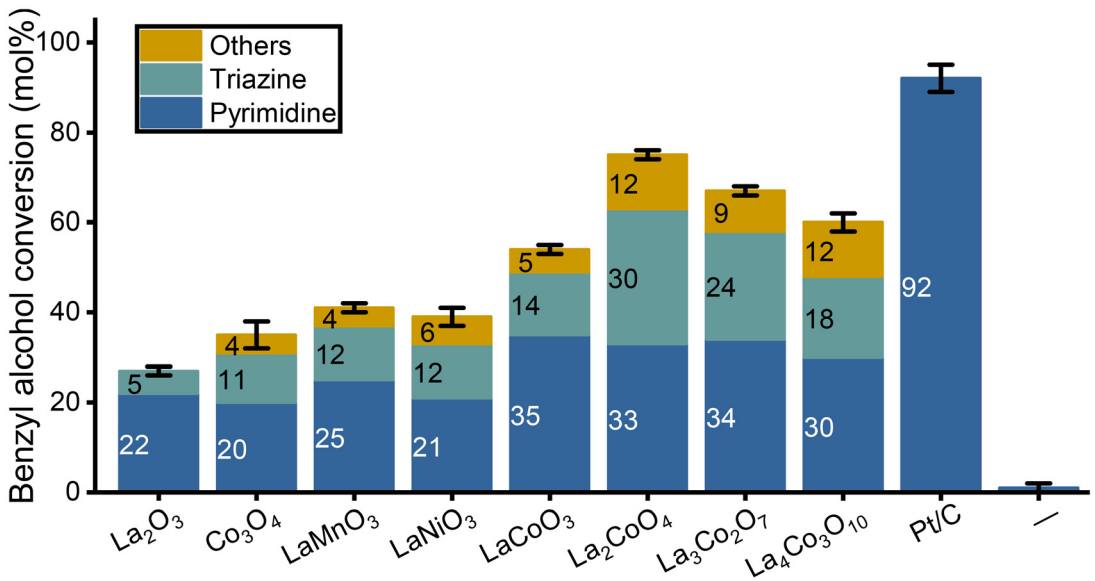

Fig. 2 ADC reaction of benzyl alcohol (0.25 mmol), phenyl ethanol (0.25 mmol) and benzamidine hydrochloride (0.25 mmol) in the presence of 2 eq. ^{t}BuOK and 10 mol% of various potential catalysts. Reaction conditions: reflux temperature, toluene of 2 mL, t = 24 h under a N_2 atmosphere.

tenance of the catalytic ability of the transition metal ions despite their insertion into the perovskite structure, which were clearly demonstrated as framework cations in pincer and other cooperative complexes. One can readily recognize simple trends in the catalytic performance of the perovskites as determined by their own composition. First, the performance of the cobalt-containing oxide (54 mol% conversion; 65 mol% selectivity) far exceeded that of their nickel- (39 mol% conversion; 54 mol% selectivity) and manganese-containing (41 mol% conversion; 61 mol% selectivity) counterparts. Second, all RP-phase variants (Fig. 2, Fig. S3) of the perovskites appeared to be more active than their perovskite-phase versions (*e.g.* Co-perovskite: 54 mol%; Co-RP: 60–75 mol%), albeit with reduced product selectivity (Co-perovskite: 65 mol%; Co-RP: 20–50 mol%). Third, a clear trend in the yield of the pyrimidine was outlined, which can be depicted in decreasing order with increasing number of metal centers in the homologous series of RP. Moreover, when testing pure transition metal oxides, that serve as building blocks in perovskites (Fig. 2, Fig. S3), very different catalytic performances were observed compared to perovskites. In each case, this meant an increase in by-products, especially triazine, with simultaneously decreasing benzyl alcohol conversions compared to the catalytic performance of the perovskites. Based on these results, it became clear that the lanthana framework does not only play a passive role as a carrier. As can be seen in Fig. 2, La_2O_3 (27 mol% conversion) has a measurable, albeit lower activity than mixed oxides in this reaction. However, the selectivity of this oxide towards the pyrimidine product is more unique (80 mol%) than that of the perovskites (55–70 mol%), indicating a crucial role of the support framework, especially in ruling the selectivity of the oxides.

The TEM (Fig. S4) measurements confirmed that not only the primary crystallite size, but also the secondary size of the structures are in the same size range (in the case of perovskites), which excludes the dependence of the differences in catalytic performance of the different oxides presented above on their own size. Like that, no remarkable difference in the – otherwise very low – specific surface areas (18–55 $m^2\ g^{-1}$) was determined using BET (Table S1). All this indicates that the observed differences must be related to the different catalytic abilities of the transition metal centers and/or structural changes depending on the physico-chemical characteristics of the guest TM or host lanthanum cations.

2.2. Optimization studies and catalytic performance of the perovskites

After proving the correctness of our hypothesis, the study was continued to find out whether perovskites are able to compete

with noble metal catalysts, which are only known for efficient heterogeneous ADC reactions. For this purpose, the optimal reaction conditions for this type of ADCs had to be found. We performed optimization experiments with $LaCoO_3$, which seemed to be more attractive than Ni- and Mn-containing catalysts. First, a solvent screening (Fig. 3A) was performed to replace toluene and other non-green solvents (THF, 1,4-dioxane, *m*-xylene), which proved to be attractive in combination with noble metal catalysts for ADC. As far as the quality of the solvent is concerned, it would be ideal to find a green solvent that is stable under the reaction conditions and can dissolve readily the reactants but does not react with them. Therefore, the reactions were observed in heptane, ethanol, *tert*-amyl methyl ether (TAME), 2-methyltetrahydrofuran (2-Me-THF) and cyclopentyl methyl ether (CPME). The use of solvents other than toluene carry with a decrease in benzyl alcohol conversions with unchanged product selectivity, with only one exception. The perovskite showed higher activity (65 mol% benzyl alcohol conversion) in the bio-renewable 2-Me-THF than in toluene. Interestingly, the perovskite also proved to be uniquely selective (~100 mol%) for the desired product. Therefore, this aprotic polar solvent was chosen for further optimization of the coupling. Apart from the fact that 2-Me-THF is a green alternative to toluene, performing the ADC in this solvent also has other environmentally friendly properties as it has a lower boiling point (T_{boil} = 80.2 °C), at which the reaction is performed instead of ~110 °C, the boiling point of toluene. Besides, optimization steps for the reaction temperature were also conducted (Table S2, entries 1–4). Although, the use of higher temperatures as the reflux in an autoclave enables higher benzaldehyde conversions (79–89 mol%), however with remarkably reduced selectivity (54–79 mol%). In contrast, any deviation from the boiling point of 2-Me-THF into the lower temperature range resulted in a remarkable decrease in benzaldehyde conversion (30 mol%). Therefore, the reflux temperature was still used for further testing. It was also found that reactions catalyzed by perovskites do not require an inert atmosphere, as the catalytic markers are not altered in reactions under an air atmosphere (pyrimidine yield of 65 *vs.* 64 mol%, Table S2; entry 5). Accordingly, air atmosphere was used for further experiments.

By changing the added base component (Table S2, entries 6–9), it was found that no other inorganic salt is suitable to promote cyclization at this level of ^{t}BuOK (23–43 mol% *vs.* 65 mol% product yield). Even when a mixture of ethanol and 2-Me-THF is prepared (Table S2, entries 10–14), all carbonates, especially cesium carbonate (52 mol%), work better compared with ^{t}BuOK (44 mol%). This is possibly related to the pure solubility of these salts in the reaction medium, which can improve immediately in the presence of aliphatic primary alcohol.[25] However, we continued with the original base, as the absolute yields from the ^{t}BuOK-assisted reaction remained higher in pure 2-Me-THF than it was possible to obtain in the solvent mixture with any base. Noticeably, the introduced reaction can work with the same efficiency when using 1.5 equivalent ^{t}BuOK (Table S2, entries 15–17) to benzyl alcohol instead of 2 equivalents which means a remarkable decrease in the amount of inorganic waste remained after the reaction.

When the ratio of the reactants was systematically varied, the significant dependence of the catalytic markers on the relative ratio of benzamidine was readily recognized (Table S2, entries 18–21). When using an alcohol excess in relative pro-

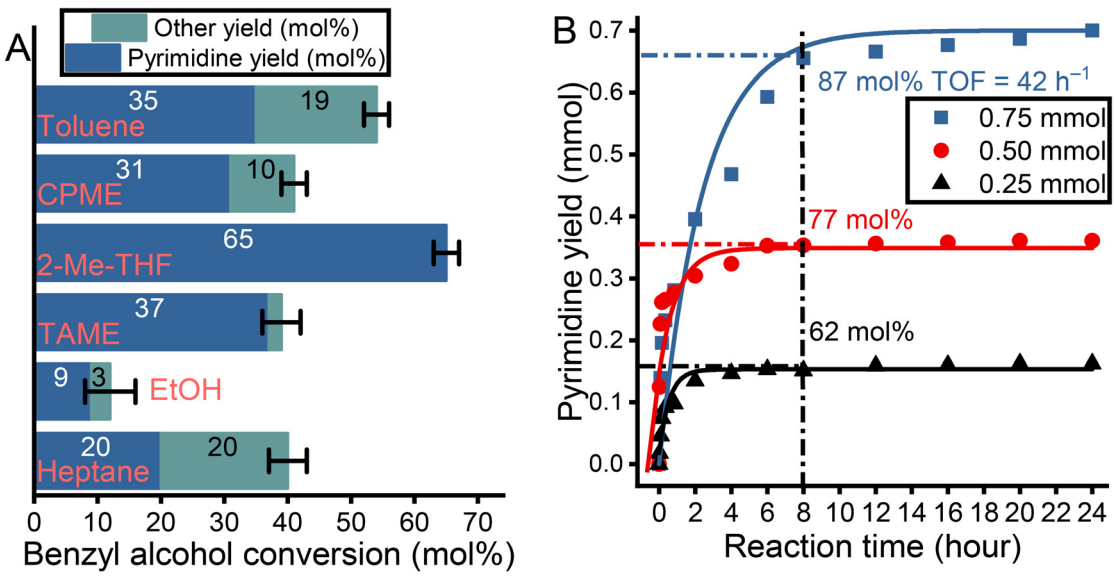

Fig. 3 Optimization of the reaction parameters for heterogeneous ADC reaction catalyzed by $LaCoO_3$. (A) Solvent screening and (B) parallel optimization of reaction time and reactant concentrations. Reaction conditions: benzyl alcohol (0.25 mmol (A)), phenyl ethanol (0.25 mmol (A)) and benzamidine hydrochloride (0.25 mmol) in the presence of 2.0 eq. (A) or 1.5 eq. (B) ^{t}BuOK and 10 mol% (A) or 5 mol% (B) of $LaCoO_3$, reflux temperature, 2-Me-THF (solvent (A)) of 2 mL, t = 24 h (A) under an air atmosphere.

portion, the indicated pyrimidine yields begin to increase in the presence of the catalyst (78–86 mol%). However, this process would have left a considerable amount of waste alcohol. Given the need to realize a reaction sequence that meets the requirements of green chemistry, the use of reactions with reduced benzamidine content was avoided. Increasing the relative ratio of benzamidine led to an opposite effect with reduced pyrimidine yields (29–35 mol%) and the appearance of a large amount of triazine and other by-products. Therefore, the use of the equimolar ratio of the substrates was maintained.

Next, the impact of catalyst loading on catalytic performance was investigated (Fig. S5). The maximum value of pyrimidine yield as a function of catalyst loading was a saturation curve. The maximum value of the plateau was reached with at least a catalyst loading of 5 mol%, which is considered optimal. However, this amount of catalyst that had to be used justified the fine-tuning of the concentration of the reactants to avoid the diffusion inhibition that might occur. As can be seen in Fig. 3B, which shows the kinetic curves of the catalytic reactions with different substrate concentrations, the conversions increased with increasing concentration of the reactants. The conversion did not further grow after a 3-fold increase in concentrations (Fig. S6). Fortunately, there were no concomitant changes in product selectivity. In all cases, the kinetic curves can be readily fitted by assuming pseudo-second order kinetics. Consequently, the minimum reaction time required to obtain the maximum yield of pyrimidine was determined to be 8 hours.

After this optimization procedure, the pure perovskites (including those containing Co, Mn and Ni) and Pt/C catalyst as a benchmark one were tested again under the optimized reaction conditions (Fig. 4A). The Ni perovskite structure still proved to be less efficient. In contrast, a benzyl alcohol conversion of 85 to 90 mol% in combination with the desired product selectivity of 100 mol% could be achieved with Co- and Mn-perovskite catalysts, respectively. In addition, $LaCoO_3$ proved to be highly active in this transformation (Fig. 4B; TOF value: 42 h^{-1}) and thus outperformed all competitors (Fig. 4B; 3–25 h^{-1}), including the Pt/C system. For perovskite structures, dynamic light scattering (DLS) studies showed no difference in the surface extension of the oxide aggregates in 2-Me-THF. This was confirmed by detecting nearly the same solvodynamic diameter for all aggregates (800–900 nm, Table S3). Therefore, the observed differences arise from the altered catalytic ability to promote the test reaction.

This performance seems to be really impressive, considering that a similar high performance can only be achieved with benchmark catalysts (Table S4) from an efficiency point of view (87 mol% product yield selectively). Furthermore, these benchmark catalysts are able to function at such a high level under harsh reaction conditions, such as reaction temperature of 105–140 °C in toluene or 1,4-dioxane over a 20–24 hours run under an inert atmosphere, with a considerable amount of waste as an excess of alcohol has to be used. All this means that the perovskite-catalyzed process must be considered as a real alternative to the well-recognized benchmark heterogeneous and homogeneous ADC processes (Table S4).[14,15,21,23,25,30] The results also align with studies indicating that bio-based N-heterocycles can be produced *via* multicomponent reactions using transition metal catalysis.[39,40] However, this requires prop-

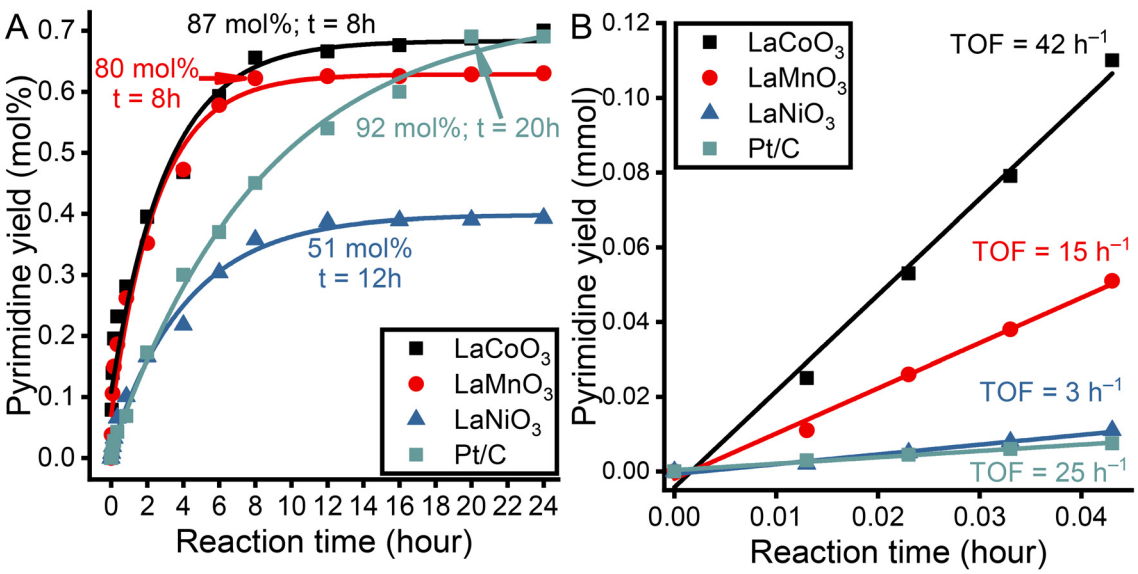

Fig. 4 Comparative kinetic analysis of the catalytic performance of the as-prepared perovskite oxides and Pt/C benchmark catalyst (A) and determination of TOF values (B) for these structures in pyrimidine synthesis *via* heterogeneous ADC cyclisation as test reaction. Reaction conditions for perovskites: benzyl alcohol (0.75 mmol), phenyl ethanol (0.75 mmol) and benzamidine hydrochloride (0.75 mmol) in the presence of 1.5 eq. ^{t}BuOK and 5 mol% of various perovskite catalysts, reflux temperature, 2-Me-THF of 2 mL, t_{max} = 24 h under an air atmosphere. Reaction conditions for Pt/C: benzyl alcohol (1.5 mmol), phenyl ethanol (1.25 mmol) and benzamidine hydrochloride (1.00 mmol) in the presence of ^{t}BuOK of 1.5 mmol and 1 mol% of Pt/C catalyst, reflux temperature, toluene of 2 mL, t_{max} = 24 h under a N_2 atmosphere.

erly designed, cooperatively functioning catalysts. In order to quantify the difference between the commonly used Pt/C and $LaCoO_3$ perovskite from an environmental point of view, the isolated yield and EcoScale[41] (Table S5) were determined for both under the different optimal reaction conditions. As can be seen, an isolated yield of 84% was achieved for the reaction promoted by perovskite and 88% for that promoted by Pt/C matching highly. Even more interesting is that the EcoScale of 81 is associated with the perovskite-promoted system, as opposed to that of 64 for the Pt/C-promoted reaction. This reflects the truly green nature of the process presented, which far outperforms the Pt/C-based method.

2.3. Understanding the catalytic performance of the simple and layered perovskites

Focusing primarily on Co-containing perovskite, which have been shown to be efficient catalyst, and their RP-phase, layered counterparts, we attempted to understand the function of these catalysts and to decide whether these mixed oxides can be considered as cooperative catalysts as envisioned. Kinetic curves (Fig. 6B and S7) and TOF values were determined/calculated for both the perovskite structures and the monometallic oxide building blocks of the oxides as well as for their physical mixture. The building block specimens of the perovskites were identified by XPS measurements (Fig. S7). Fig. S7A shows that on the surface of the perovskites predominantly Co(III) centers (80–85% of the total cobalt) co-exist with neighboring oxygen-containing specimens and – to a much lesser extent – Co(II) centers (15–20%) in combination with oxygen vacancies. In addition, La(III) centers (Fig. S7B) are also found without La(II) sites in a local environment identical to that in a lanthana structure. Consequently, commercially available La_2O_3, CoO and Co_3O_4 were included as models in the tests.

First of all, based on the comparative catalytic tests summarized in Fig. 5, it can be stated that in the absence of the catalyst, there was a measurable benzyl alcohol conversion (10 mol%), though in combination with non-selective character (47 mol%). This low level conversion can be associated with an alternative, ^{t}BuOK-promoted pathway previously reported under aerobic conditions.[42] Second, there were no significant changes in the catalytic markers either in the presence or absence of the CoO structure, which proves the catalytic inactivity of this specimen (Fig. 5). Both lanthana and Co_3O_4 allow this cyclization, but with low activity (4–12 h^{-1}). In Fig. 5, we can see that Co_3O_4 is able to accelerate the test reactions in a selective manner (pyrimidine selectivity: 80 mol%), in contrast to lanthana, which only has pure selectivity (48 mol%) but a higher activity. This improved selectivity of the TM oxide was partly transferred to the lanthana/TM physical mixture (70 mol%), which is accompanied by a slightly increased activity, although this is still far from that of the perovskites (21 h^{-1}). However, the perovskite structure outperformed the tested physical mixture and the monometallic oxides in all catalytic markers (42 h^{-1}, 87 mol% conversion and 100 mol% selectivity). This suggests that there may be a synergistic effect between lanthana and TM oxide sites in perovskites. To decide whether a true synergism could be formed or not, a two-way ANOVA analysis[43] of the pyrimidine yield data was performed (Fig. 6A). This showed the additive or possibly antagonistic nature of the activity of the oxides when using the mixing process. In sharp contrast, it was also properly pointed out that there must be a synergistic effect between lanthana and TM units in perovskites. This suggests that

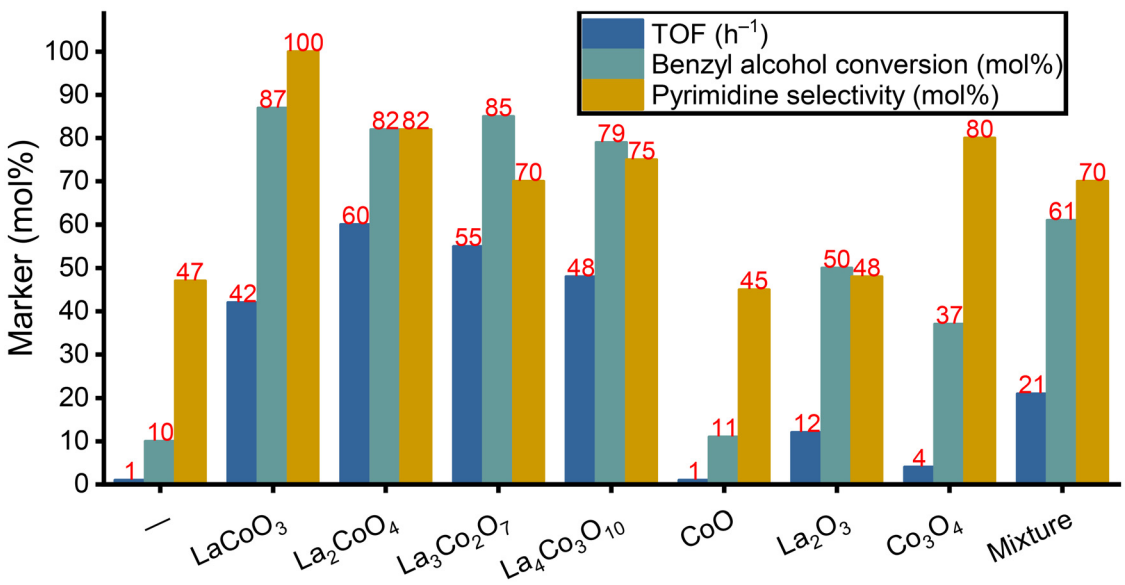

Fig. 5 Catalytic performance of the as-prepared monometallic and bimetallic La/Co oxides in ADC test reaction. Reaction conditions: benzyl alcohol (0.75 mmol), phenyl ethanol (0.75 mmol) and benzamidine hydrochloride (0.75 mmol) in the presence of 1.5 eq. ^{t}BuOK and 5 mol% of various oxide catalysts, reflux temperature, 2-Me-THF of 2 mL, t_{max} = 24 h under an air atmosphere.

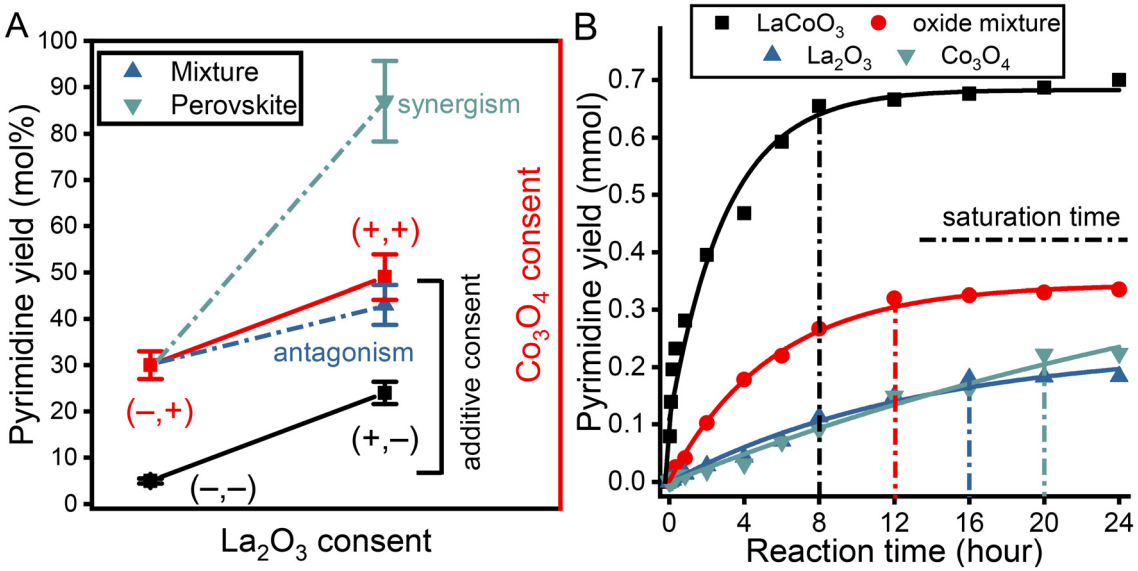

Fig. 6 Two-way ANOVA analysis of La/Co oxide system to decide the existence of the synergistic catalytic effect between lanthana and Co_3O_4 units on a perovskite surface (A). Kinetic curve of the ADC test reactions catalyzed by the as-prepared monometallic and bimetallic La/Co oxide catalysts (B). Reaction conditions: benzyl alcohol (0.75 mmol), phenyl ethanol (0.75 mmol) and benzamidine hydrochloride (0.75 mmol) in the presence of 1.5 eq. ^{t}BuOK and 5 mol% of various oxide catalysts, reflux temperature, 2-Me-THF of 2 mL, t_{max} = 24 h under an air atmosphere.

lanthanum oxide and TM oxide units are working cooperatively on the surface of the perovskites. This was further strengthened by the kinetic curves of the reactions catalyzed by the tested oxides (Fig. 6B). Indeed, depending on the quality of the catalysts, not only the maximum yield (24–87 mol%) possible to reach but also the sufficient time to obtain the saturation plateau (8–20 hours) change remarkably. This clearly demonstrated the real difference in the catalytic performance of the mixture and perovskite double oxides.

Furthermore, the present results suggest that the lanthana centers dictate the activity evolution, while the TM oxide moieties are responsible for the selectivity of the solid. To corroborate this finding, RP phase oxides were also included in these tests (Fig. 5), as they have a much different surface composition from simple perovskites. In all cases, RP-phase oxides have a higher catalytic activity according to TOF values (48–60 h^{-1}, Fig. 5) than their non-layered counterpart (42 h^{-1}). In addition, the required reaction time for saturation of the kinetic curves is significantly reduced (6 h; Fig. S8) when RP phases were used compared with simple perovskites (8 h). In contrast, the selectivity of these systems decreased to the range of 70–82 mol% for the desired product, which is an apparent contradiction since the ratio of the putative selectivity controller TM specimens is higher in the RP-phase oxides than in the pure perovskite. As for the performance in the homologous RP series, according to the reported turnovers and selectivities, there seems to be a regular decrease in the markers monitored, following the decrease in the actual La/Co ratios. This latter trend would also not fit well with our assumption, as the decrease in the ratio of the lanthana specimens should lead to a decrease in the activity of the solids.

However, the XPS measurements exhibit that the surface composition of the RP phase oxides does not match the theoretical and bulk composition and shows a clear excess of La (Fig. 7A). Consequently, the strong decrease in the selectivity of the structures can be linked to the strongly reduced Co/La ratios on the surface of the RP phases compared to those of the simple perovskite structure. However, it remained an open question why the activity in the homologous series decreases, although the ratio of lanthanum sites increases significantly. At this point, it was assumed that the differences in surface acidity should have a decisive impact on the catalytic activity.[29] This assumption was confirmed by the NH_3–TPD results (Fig. 7B and C). Although the acid strength distribution is almost the same for all perovskite derivatives, large differences in the amount of adsorbed ammonia were observed. While the simple perovskite structure can adsorb ammonia in an amount of 205 μmol per gram, the RP-phase oxides adsorbed ammonia in an amount of 1300–2000 μmol per gram. Furthermore, the changes in the amount of adsorbed ammonia show exactly the same order of the perovskite derivatives as established based on their catalytic activity according to TOF values (Fig. 5). Therefore, the activity of the perovskites is possibly governed by their own surface acidity. To understand the experienced trend, we measured the acidity of both La_2O_3 and Co_2O_3 structures using NH_3–TPD measurements (Fig. S9). Co_2O_3 adsorbed a higher amount of the probe molecule (490 μmol g^{-1}) than La_2O_3 (140 μmol g^{-1}). This appears to contradict our results, because we observed an increase in acidity with a decreasing number of cobalt sites in the RP phase structures. However, previous studies have shown that the strength of isolated active Lewis acid sites can be higher

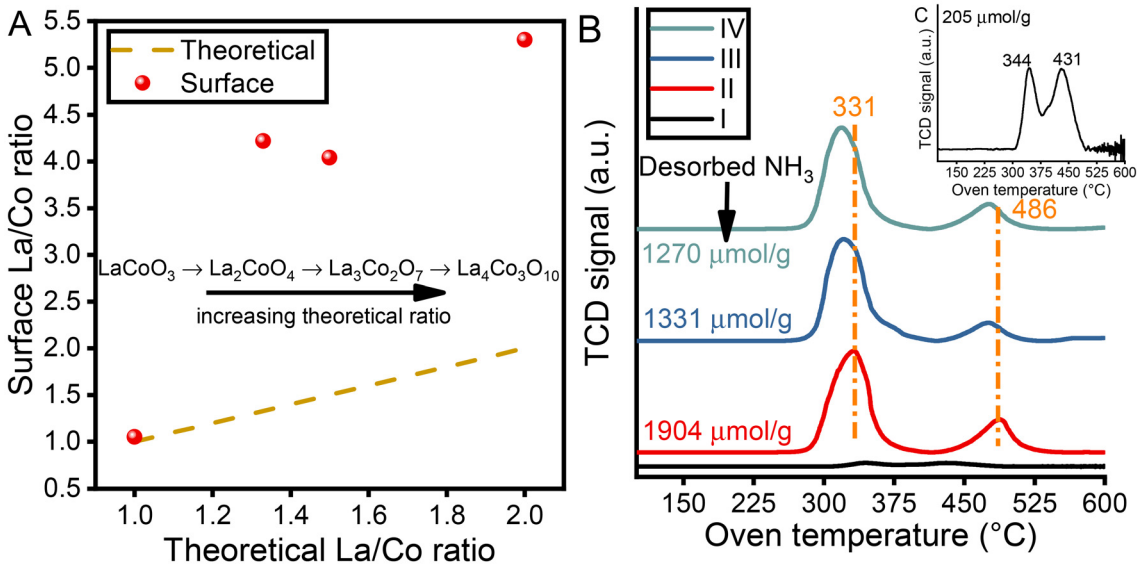

Fig. 7 Actual La/Co ratios on the surface of the corresponding perovskite oxides determined by XPS analysis in comparison to the theoretical ratios (A). NH_3–TPD profile of the corresponding perovskites (B; I: $LaCoO_3$; II: La_2CoO_4; III: $La_3Co_2O_7$, IV: $La_4Co_3O_{10}$). NH_3–TPD profile of $LaCoO_3$ (C).

than that of conjugated ones.[44] Since the number of cobalt sites decreases with increasing Co/La ratios in RP phase systems, these sites become more isolated than those on the surface of pure perovskite. Therefore, their strength may be enhanced, which could explain the observed trend.

2.4. Mechanistic investigation and control experiments

To identify the corresponding sub-steps in the catalytic cycle possibly promoted by different parts (lanthana or TM specimens) of the perovskites, control experiments were performed (Scheme 2), assuming that the proposed mechanism known for homogeneously catalyzed pyrimidine synthesis by the ADC mechanism (Scheme S1) can also be applied to perovskite-catalyzed reactions. In the first step of this classical ADC mechanism, dehydrogenation of both alcohol reactants takes place with the liberation of hydrogen, followed by cross-aldol condensation of the carbonyl compounds generated *in situ*, yielding an α,β-unsaturated ketone (chalcone). This reacts with benzamidine *via* a cyclization reaction in which new C–N bonds are formed. The resulting condensation product undergoes a further dehydrogenation/hydrogen release reaction in the final step of the cycle, which yields the pyrimidine as the final product.[30]

This mechanism shows that the catalytic ability of perovskites and monometallic oxides must be investigated in three different reactions to obtain a clear picture. First, the acceptorless dehydrogenation of both phenyl ethanol (Scheme 2/**1**) and benzyl alcohol (Scheme 2/**2**) with the mentioned oxides was attempted. With all three structures, both reactions can be completed with different efficiencies. Based on 4-hour-long runs, the structures can be arranged in the order perovskite > La(III) oxide > Co(II/III) oxide by decreasing alcohol conversions. In the case of the benzaldehyde reactant, however, three different product distributions were obtained. While a mixture of benzoic acid and benzaldehyde was formed in the presence of perovskite and cobalt(II/III) oxide, benzaldehyde was the almost only detectable product formed by lanthana catalysis (95 mol% selectivity). This is due to the ability of the TM (mixed) oxides to overoxidize benzaldehyde with the aid of molecular oxygen under aerobic conditions. A similar effect was not observed for acetophenone, whose overoxidation is not thermodynamically favored. Noticeably, due to its strong Lewis acid character, La(III) oxide can promote the aldol self-condensation of acetophenone. Therefore, the lanthana specimens on the surface of the perovskites are possibly responsible for avoiding overoxidation of benzyl alcohol as much as possible in this reaction step. When repeating the experiments under a N_2 atmosphere (Scheme 2/**3**), all three solids exhibit unique benzaldehyde selectivity, which is consistent with the hypothesis of overoxidation ability of the TM specimens.[45] Second, the cross-aldol condensation of carbonyl compounds to chalcone (Scheme 2/**4**) appears to be a key step from a selectivity perspective. Lanthana is able to promote this condensation with high activity (68 mol% conversion) in a selective manner (100 mol%). The high selectivity is likely related to the relatively strong Lewis acid character of lanthana. On the contrary, both Co-containing systems also afforded the aldol condensation product, albeit with reduced activity (38–48 mol%). Furthermore, we repeated these tests in the presence of benzamidine (Scheme 2/**5**) and lanthana, directly yielding triazine (53 mol% triazine selectivity) – the most common by-product of the cyclization – as the major product and pyrimidine as the minor product. This competing reaction, in which triazine is formed (Scheme S1), takes place when the aldehyde reacts directly with the amidine to form carboximidamide, which, on further reaction with the amidine

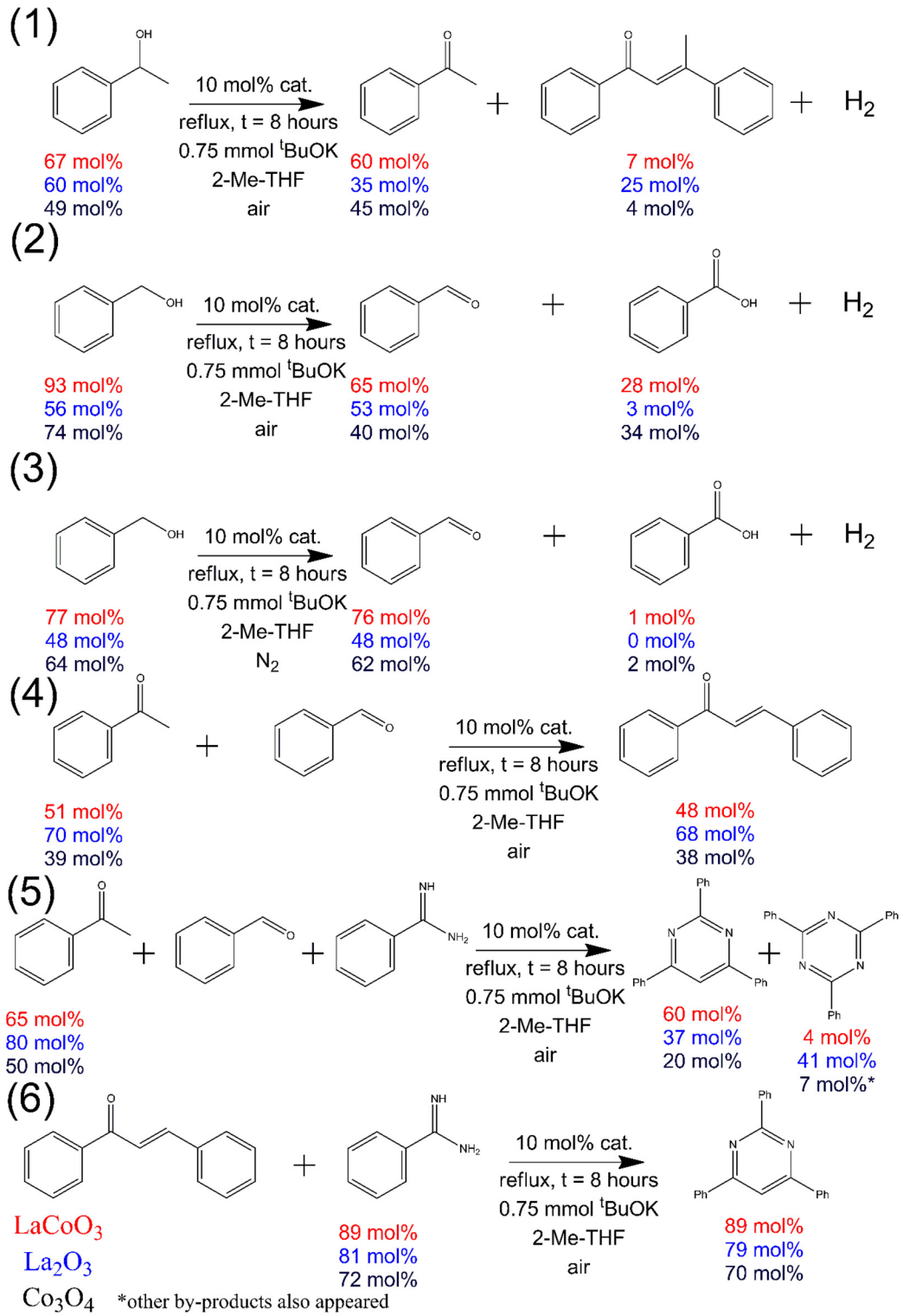

Scheme 2 Control experiments.

gives dihydrotriazine. The by-product triazine can be produced by dehydrogenation of dihydrotriazine. Using perovskite catalysis, a product mixture of pyrimidine and triazine can be obtained in a ratio of 9 : 1, albeit with reduced conversions. This reflects well the controlling role of the TM specimens on the catalyst surface and also indicates that the dehydrogenation of the alcohols is the rate-determining step controlled by the activity of the lanthana specimens having providing really high conversion (80 mol%), which is in good agreement with our results. It was also found that pure cobalt oxide exhibits

significantly lower activity in both cyclization and subsequent dehydrogenation to give a mixture of chalcone, dihydropyrimidine and pyrimidine, confirming the latter observation. Finally, all three solids are able to fully selectively promote the reaction of chalcone and benzamidine to the desired product (Scheme 2/**6**). It is noticeable that, based on the given chalcone conversions, there is a remarkable difference in the activity of the solids used by what has been described above.

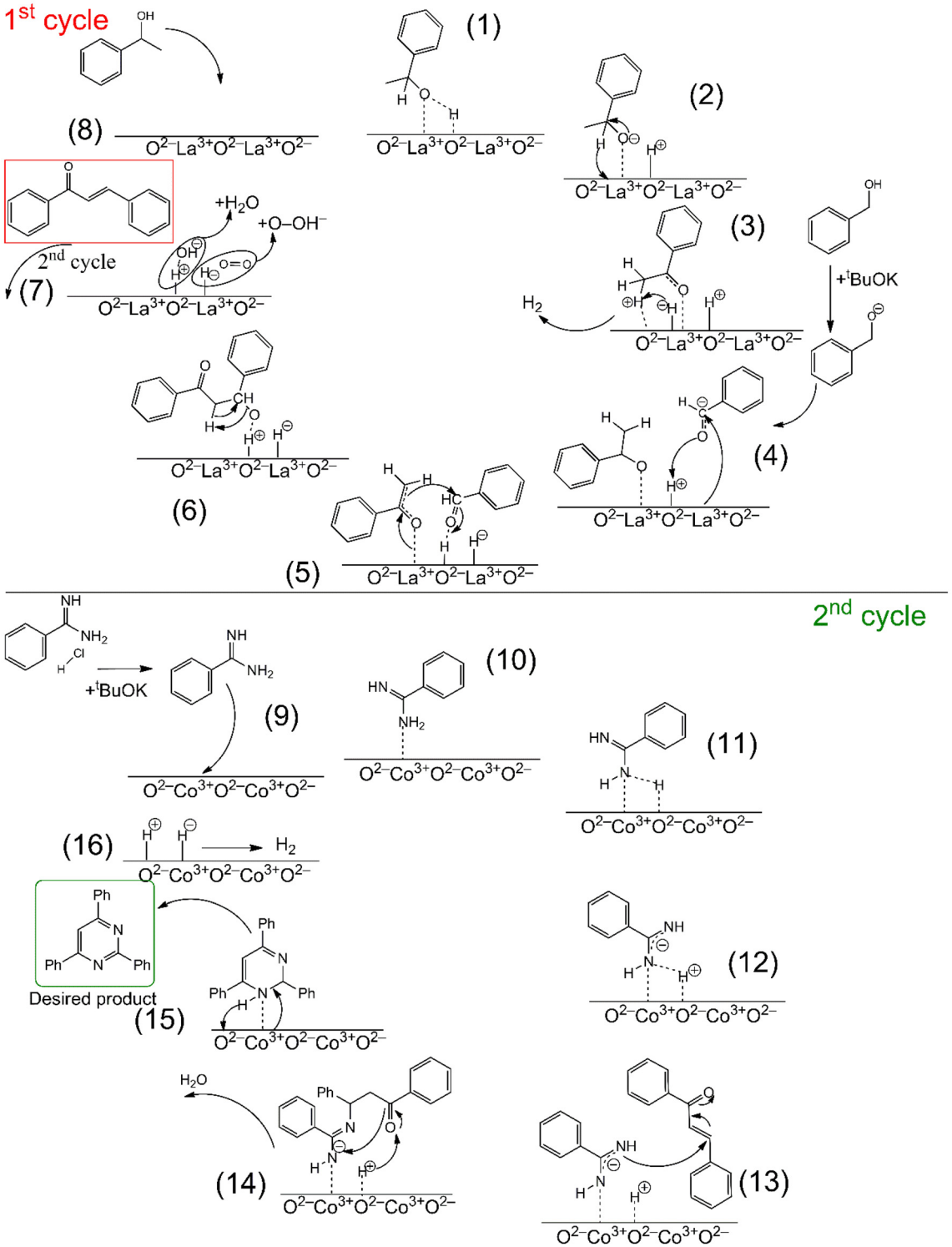

Scheme 3 Proposed mechanism of oxidative dehydrogenative coupling reaction of phenyl ethanol, benzyl alcohol and benzamidine hydrochloride catalyzed by $LaCoO_3$, providing pyrimidine.

Given the results of the control experiments and previously showcased reaction mechanisms,[30,32,46–48] the most probable but simplified reaction mechanism is proposed (Scheme 3). We have envisioned a tandem working mechanism consisting of two cycles. In the first step of the first cycle **(1)**, the phenyl ethanol molecule adsorbs with its alcoholic oxygen at a La(III) site and forms a quasi-lanthanum alkoxide surface specimen. Subsequently, proton abstraction occurs from the alcohol group of the reactant **(2)**, which is reacted by a neighboring lattice oxide anion (O^{2-}). Then, β-H elimination takes place, which is promoted by La(III) sites and leads to the formation of La(III) hydride specimen **(3)**. The highly reactive hydride specimen immediately extracts an α-hydrogen as a proton, and a surface-adsorbed enolate is formed **(3)**, while hydrogen liberation occurs *via* an umpolung mechanism.[49] Meanwhile, in the fourth step **(4)**, ^{t}BuOK abstracts a proton from the alcohol group of the benzyl alcohol, and subsequently the carbonyl group – which exists in a resonance structure of the generated alcoholate – can adsorb to the *in situ* generated hydroxyl group on the surface (see above). This is followed by a further β-H elimination, which produces the activated benzaldehyde adsorbed on the surface **(4)**. In the fifth step **(5)**, the nucleophilic enolate attacks the activated benzaldehyde to generate a new C–C bond leading to a β-hydroxy ketone on the surface, which can rearrange by a nucleophilic attack of the hydroxyl oxygen on the ketonic α-hydrogen **(6)**. This leads to the formation of chalcone, which is desorbed similar to a water molecule formed by the rearrangement on the surface **(7)**. Finally, La(III)-hydride reacts with molecular oxygen to form peroxide anion, and the original catalyst surface is regenerated.[32,46] The degradation of peroxide anion has already been demonstrated by Riisager *et al.*[46] In parallel, in the second cycle, the hydrochloride is extracted from the benzamidine salt by the ^{t}BuOK base **(9)** and the benzamidine adsorbs at the Co(III) sites, forming a bond *via* its secondary amino group **(10)**. Thereafter, a surface oxide anion (O^{2-}) abstracts a proton from the secondary amino group of the amidine, enabling the formation of the amidine anion **(11, 12)**.[48] This strongly nucleophilic agent immediately attacks the desorbed chalcone **(13)**, which was formed in the first cycle (nucleophilic addition). This leads to an addition adduct, which is stabilized by a water elimination step **(14)**. Finally, a dehydrogenative desorption/cyclization takes place **(15)**, yielding the pyrimidine final product and another hydrogen molecule *via* an umpolung reaction **(16)** while the original oxide surface is regenerated.

2.5. Reusability and heterogeneity tests of the perovskites

To investigate the stability and recyclability of the $LaCoO_3$ catalyst, a series of recycling experiments were carried out. Specifically, the catalyst was removed from the reaction mixture by centrifugation after an 8-hour-long run. The same spent batch was then thoroughly washed to remove organic impurities from the surface of the perovskite, dried overnight in an oven, and reused in another cycle under the optimized reaction conditions. The catalyst markers were continuously monitored (Fig. 8A). The obtained TOF values, selectivity and pyrimidine yields show no remarkable changes in catalyst activity even after eight consecutive runs. After the eighth cycle, a slight decrease in catalytic markers can be observed (9–11th runs). This decrease can readily be linked to the KCl contamination confirmed by XRD (Fig. S10), which is enriched on the catalyst surface after eight runs and possibly blocks at least part of the active sites. Both NH_3–TPD and BET studies were conducted on the spent catalyst after the eighth cycle (Table S6). While the accessible surface acidic sites of $LaCoO_3$ decreased to half of the original value (110 μmol g^{-1} NH_3),

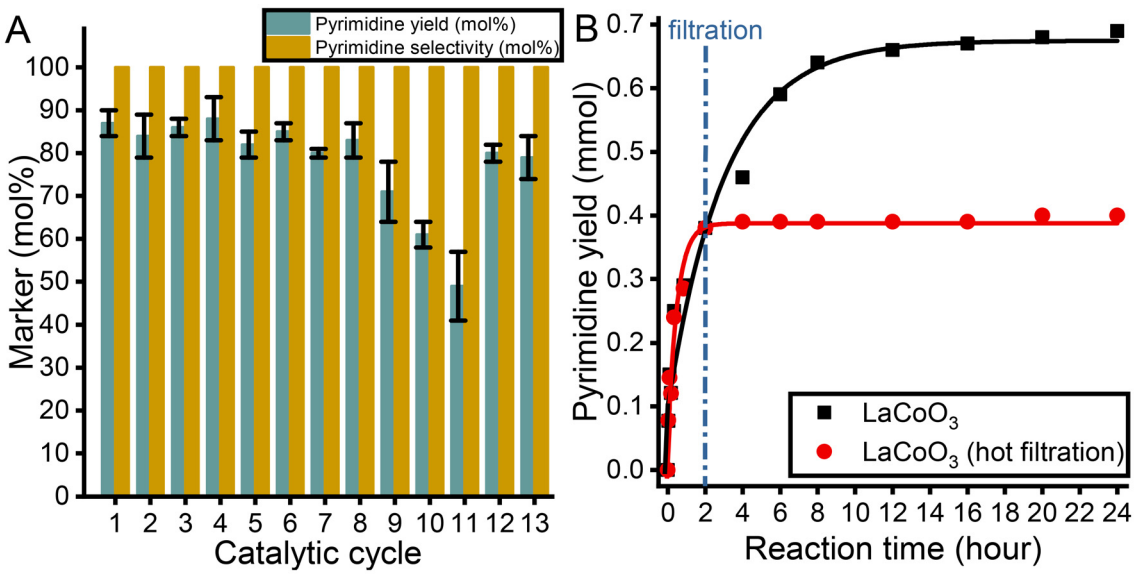

Fig. 8 Recycling tests (A) and the hot filtration test (B) of $LaCoO_3$ catalyst. Reaction conditions: benzyl alcohol (0.75 mmol), phenyl ethanol (0.75 mmol) and benzamidine hydrochloride (0.75 mmol) in the presence of 1.5 eq. ^{t}BuOK and 5 mol% of $LaCoO_3$, reflux temperature, 2-Me-THF of 2 mL, t = 8 h (A) under an air atmosphere.

only a slight decrease in the specific surface area was observed (33 $m^2 g^{-1}$ compared to the original 40 $m^2 g^{-1}$). This indicates that the acid site density decreased due to KCl contamination. Fortunately, the catalyst can be regenerated by boiling in hot water and drying in vacuum, whereupon the catalytic markers were restored (12–13th cycles). Leaching of the active com-

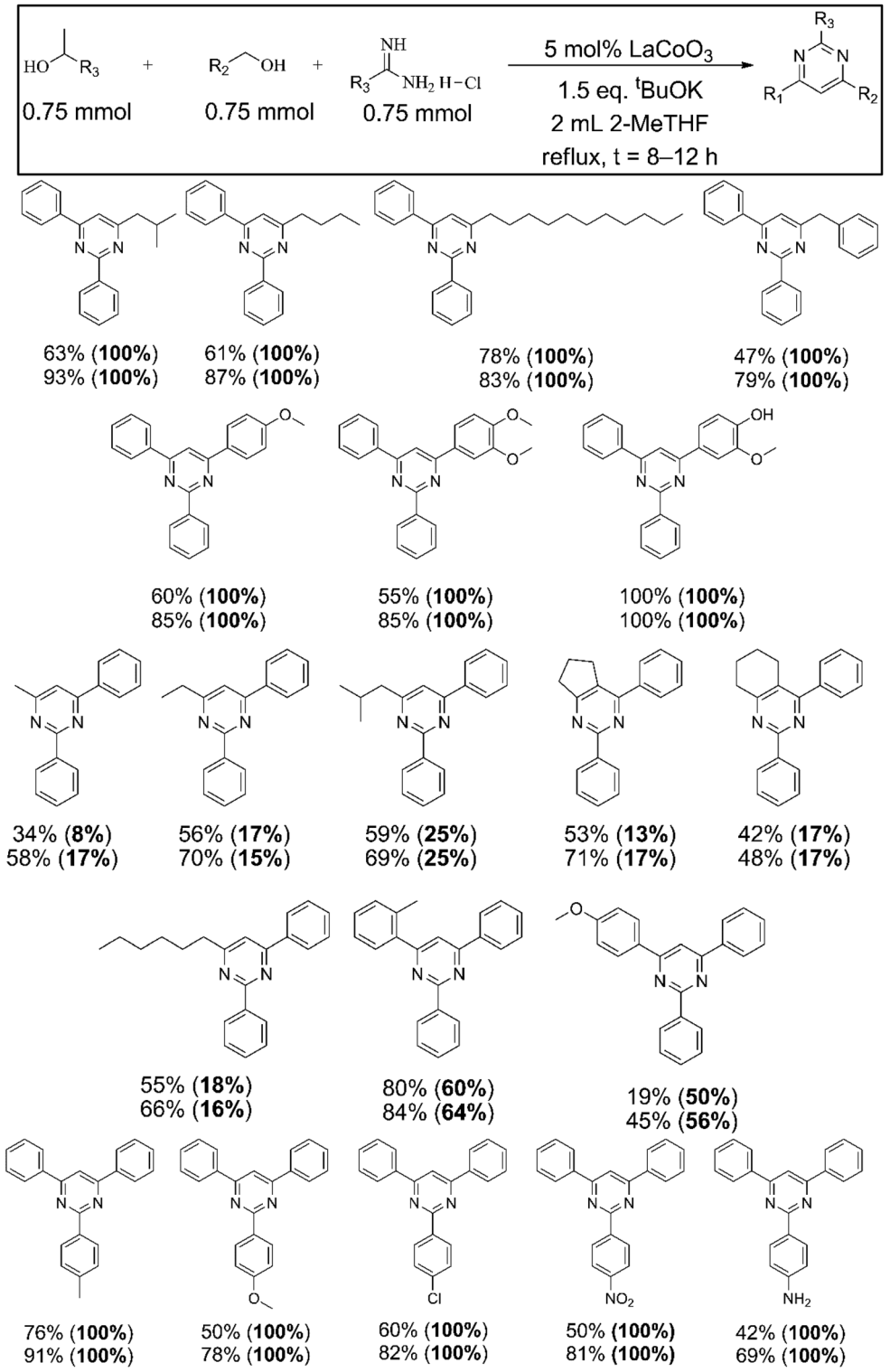

Scheme 4 Synthesis of pyrimidines from differently substituted reactants. Reaction parameters: primary alcohol (0.75 mmol), secondary alcohol (0.75 mmol) and amidine (0.75 mmol) in the presence of 1.5 eq. ^{t}BuOK and 5 mol% of $LaCoO_3$, reflux temperature, 2-Me-THF of 2 mL, t = 8 h (upper values) or t = 12 h (lower values) under an air atmosphere. Selectivity data can be found in the brackets.

ponents was also monitored by analyzing the crude products – after removal of the solid catalyst – using ICP-MS technique. No leaching within the detection limit of the method was observed during the recycling tests.

To consider the $LaCoO_3$ structure as a heterogeneous catalyst, the heterogeneity of the catalytic reaction must be demonstrated (Fig. 8B). For this purpose, a hot filtration test was carried out. In the test, two reaction mixtures loaded with $LaCoO_3$ of the same batch were compiled and treated under the optimized reaction conditions. After reaching a pyrimidine yield of ~40 mol% – approximated by the measured kinetic curve (see above) – the reactions were cooled to room temperature. The catalyst was then removed from one of the mixtures by centrifugation. The mixtures were then treated again under the same reaction conditions before being cooled. Comparing the obtained kinetic curves with each other, it seems clear that the reaction cannot continue at all after removing the catalyst from the system. On the contrary, the second, comparative reaction can be completed despite the cooling. All this means that the Co-containing perovskite is apparently also recyclable and heterogeneous and thus meets the requirements for environmentally friendly catalytic processes.

2.6. Substrate scope of the reaction

In addition to the really important characteristics of catalysts, from selectivity to activity, the generality or versatility of the catalytic process developed is of great importance from an economic point of view. To showcase the versatility of the perovskite catalyst, various test reactions were carried out in which the quality of the substrates was varied (Scheme 4). When using substituted secondary alcohols and benzamidines, only pyrimidine derivatives (100 mol%) can be produced in combination with moderate to excellent substrate conversions (47–100 mol%). When the reaction time is increased to 12 hours, conversions can range from good to excellent (75–100 mol%). However, varying the substitution of the primary alcohol resulted in a significant decrease in catalytic markers (34–80 mol% conversions; 15–60 mol% selectivity). We also tried to increase the reaction time in this case (t = 12 hours), but only a moderate increase in markers was observed (58–84 mol% conversion, 15–64 mol% selectivity). When using primary alcohols with similar polarity to benzyl alcohol, such as 2-phenylethanol, 2-phenoxyethanol, and 3-phenylpropanol, similarly high levels of the markers (conversion of 85–92 mol% and selectivity of 95–100 mol% for the desired product) were observed as in the benzyl alcohol-containing system (Table S7). Based on these results, we supposed that this phenomenon is closely related to the deprotonation of primary alcohols. This step is supposed to be straightforward. However, it was previously found that ^{t}BuOK can become almost completely inactive as a base in various organic solvents (*e.g.* MeCN) under aerobic conditions.[50] Since there is no data on how this base functions in 2-Me-THF for the deprotonation of alcohols, it is difficult to determine which types of primary alcohols can be efficiently deprotonated in this medium. Nevertheless, the broad substrate tolerance is characteristic of the perovskite catalyst with a certain sensitivity to the (degree of) substitution of the primary alcohol component.

3. Conclusions

In summary, we have found that an efficient, noble metal-free heterogeneous catalytic ADC three-component cyclization of alcohols and benzamidine to pyrimidine can be realized with La-based perovskites and their RP-phase counterparts as catalysts in a selective and recyclable manner. Ni-, Mn- and Co-containing systems all showed activity in this reaction, with the latter standing out strongly from the others. By means of $LaCoO_3$ catalysis, it is possible to achieve an isolated pyrimidine yield of 84 mol% under mild reaction conditions (T = 80 °C, under an air atmosphere) in a green solvent (2-Me-THF) with a remarkably short reaction time (t = 8 h) relative to that of the benchmark reactions of noble metal catalysis (t = 20–24 h), even in eight consecutive runs. In addition, the number of runs can be increased by a simple regeneration process. The EcoScale value of 81 compared to that of 64 of the most efficient benchmark reaction, clearly shows the eco-friendly nature of this process. In addition, the Co-perovskite catalyst has a reasoning functional group tolerance that enables the cyclization of substituted secondary alcohols and benzamidines while showing sensitivity to the substituent of the primary alcohol. Furthermore, we have exhibited that in this oxide the redox-active transition metal active sites neighboring by oxide anions and lanthana centers can work cooperatively. The control of the reaction rate is attributed to the lanthana specimens, while the transition metal oxide specimens are responsible for controlling the product selectivity. Lanthana sites enable the rapid cross-aldol condensation of *in situ* generated carbonyl compounds to chalcone while avoiding their overoxidation. However, the TM sites completely prevent the formation of the triazine by-product from chalcone, which is favored by lanthana units. The whole process is strongly controlled by the acidic character of the perovskite surface from an activity point of view.

Author contributions

The manuscript was written through contributions of all authors. All authors have given approval to the final version of the manuscript.

Conflicts of interest

There are no conflicts of interest to declare.

Data availability

Supplemental data are available in the supplementary information (SI). Supplementary information: XRD patterns and

Raman spectra of perovskite and RP-phase structures; analytical data of the as-prepared structures; representative TEM images, optimization procedure of ADC reaction, XPS analysis of the as-prepared Co-containing structures. Analytical data of the synthesized pyrimidine derivatives. See DOI: https://doi.org/10.1039/d5gc04945h.

Requests for additional data or code will be fulfilled by the lead contact upon reasonable request.

Acknowledgements

G. Varga is very grateful for the financial support from the NRDI Office under a STARTING grant (project number: STARTING 15087) and from the Hungarian Academy of Science under a Bolyai Janos Research Fellowship (BO/00673/24/7).

References

1 T. Li, M. Lv, H. Wen and H. Xu, *J. Agric. Food Chem.*, 2023, **71**, 17036–17045.
2 C. M. Russo, Z. W. Boyer, K. Scheunemann, J. Farren, A. Minich, C. J. Wenthur and M. C. O'Reilly, *ACS Med. Chem. Lett.*, 2024, **15**, 1094–1101.
3 J. Chang, *Acc. Chem. Res.*, 2022, **55**, 565–578.
4 B. A. Vara, S. M. Levi, A. Achab, D. A. Candito, X. Fradera, C. A. Lesburg, S. Kawamura, B. M. Lacey, J. Lim, J. L. Methot, Z. Xu, H. Xu, D. M. Smith, J. A. Piesvaux, J. R. Miller, M. Bittinger, S. H. Ranganath, D. J. Bennett, E. F. Dimauro and A. Pasternak, *ACS Med. Chem. Lett.*, 2021, **12**, 653–661.
5 J. C. Tellis, B. Q. Wei, M. Siu, L. An, G. K. Chan, Y. Chen, X. Du, L. Gazzard, B. Hu, J. Kiefer, S. Kakiuchi-Kiyota, M. Lainchbury, J. L. Linehan, X. Luo, S. Malhotra, R. Mendonca, J. Pang, Y. Ran, V. Sethuraman, E. Seward, C. Sneeringer, D. Su, W. Wang, P. Wu, J. G. Moffat, T. P. Heffron, E. F. Choo and B. K. Chan, *ACS Med. Chem. Lett.*, 2024, **15**, 1606–1614.
6 R. S. Butler, P. Cohn, P. Tenzel, K. A. Abboud and R. K. Castellano, *J. Am. Chem. Soc.*, 2009, **131**, 623–633.
7 P. Nicolas, C. Minon, S. Abdallah, D. Chen, G. Rizzi, Y. de Coene, W. Liu, O. Jeannin, T. Verbiest, K. Clays, N. Bellec, B. Bilgin-Eran, H. Akdas-Kiliç, J. P. Malval, S. Van Cleuvenbergen and F. Camerel, *Adv. Opt. Mater.*, 2024, 2402083.
8 S. Crespi, N. A. Simeth and B. König, *Nat. Rev. Chem.*, 2019, **3**, 133–146.
9 C. M. Glinkerman and D. L. Boger, *Org. Lett.*, 2015, **17**, 4002–4005.
10 M. Movassaghi and M. D. Hill, *J. Am. Chem. Soc.*, 2006, **128**, 14254–14255.
11 J. L. Zhan, M. W. Wu, F. Chen and B. Han, *J. Org. Chem.*, 2016, **81**, 11994–12000.
12 V. K. Maikhuri, D. Mathur, A. Chaudhary, R. Kumar, V. S. Parmar and B. K. Singh, *Transition-Metal Catalyzed Synthesis of Pyrimidines: Recent Advances, Mechanism, Scope and Future Perspectives*, Springer International Publishing, 2024, vol. 382.
13 A. M. Afanasenko, N. Deak, J. October, R. Sole and K. Barta, *Green Chem.*, 2025, **27**, 5947–5981.
14 M. Mastalir, M. Glatz, E. Pittenauer, G. Allmaier and K. Kirchner, *Org. Lett.*, 2019, **21**, 1116–1120.
15 N. Deibl, K. Ament and R. Kempe, *J. Am. Chem. Soc.*, 2015, **137**, 12804–12807.
16 P. Daw, Y. Ben-David and D. Milstein, *J. Am. Chem. Soc.*, 2018, **140**, 11931–11934.
17 N. Biswas and D. Srimani, *J. Org. Chem.*, 2021, **86**, 9733–9743.
18 M. Trincado, J. Bösken and H. Grützmacher, *Coord. Chem. Rev.*, 2021, **443**, 213967.
19 R. K. Singh, D. Yadav, S. Misra and A. K. Singh, *Dalton Trans.*, 2023, **52**, 15878–15895.
20 X. Wang, C. Wang, Y. Liu and J. Xiao, *Green Chem.*, 2016, **18**, 4605–4610.
21 N. Deibl and R. Kempe, *Angew. Chem., Int. Ed.*, 2017, **56**, 1663–1666.
22 S. Chakraborty, U. K. Das, Y. Ben-David and D. Milstein, *J. Am. Chem. Soc.*, 2017, **139**, 11710–11713.
23 M. Mastalir, M. Glatz, E. Pittenauer, G. Allmaier and K. Kirchner, *J. Am. Chem. Soc.*, 2016, **138**, 15543–15546.
24 S. P. Midya, V. G. Landge, M. K. Sahoo, J. Rana and E. Balaraman, *Chem. Commun.*, 2017, **54**, 90–93.
25 C. Savarimuthu Selvan, R. Rengan and J. G. Malecki, *J. Org. Chem.*, 2024, **89**, 11148–11160.
26 A. Mondal, R. Sharma, B. Dutta, D. Pal and D. Srimani, *J. Org. Chem.*, 2022, **87**, 3989–4000.
27 Z. Shao, Y. Wang, Y. Liu, Q. Wang, X. Fu and Q. Liu, *Org. Chem. Front.*, 2018, **5**, 1248–1256.
28 K. Bera and A. Mukherjee, *Tetrahedron Lett.*, 2021, **81**, 153326.
29 S. M. A. Hakim Siddiki, T. Toyao and K. I. Shimizu, *Green Chem.*, 2018, **20**, 2933–2952.
30 S. Sultana Poly, S. M. A. H. Siddiki, A. S. Touchy, K. W. Ting, T. Toyao, Z. Maeno, Y. Kanda and K. I. Shimizu, *ACS Catal.*, 2018, **8**, 11330–11341.
31 K. I. Shimizu, K. Kon, K. Shimura and S. S. M. A. Hakim, *J. Catal.*, 2013, **300**, 242–250.
32 M. Kocsis, K. Baán, S. B. Ötvös, Á. Kukovecz, Z. Kónya, P. Sipos, I. Pálinkó and G. Varga, *Catal. Sci. Technol.*, 2023, **13**, 3069–3083.
33 A. A. Ádám, S. B. Nagy, Á. Kukovecz, Z. Kónya, P. Sipos and G. Varga, *Chem. Commun.*, 2024, 10520–10523.
34 H. Arandiyan, P. Sudarsanam, S. K. Bhargava, A. F. Lee and K. Wilson, *ACS Catal.*, 2023, **13**, 7879–7916.
35 Q. Yang, G. Liu and Y. Liu, *Ind. Eng. Chem. Res.*, 2018, **57**, 1–17.
36 S. Liu, C. Sun, J. Chen, J. Xiao and J. L. Luo, *ACS Catal.*, 2020, **10**, 13437–13444.
37 G. Koch, M. Hävecker, D. Teschner, S. J. Carey, Y. Wang, P. Kube, W. Hetaba, T. Lunkenbein, G. Auffermann,

O. Timpe, F. Rosowski, R. Schlögl and A. Trunschke, *ACS Catal.*, 2020, **10**, 7007–7020.
38 S. T. Dong, N. Sun, B. B. Zhang, F. Zhang, S. H. Yao, J. Zhou, S. T. Zhang, Z. B. Gu, Y. B. Chen and Y. F. Chen, *Mater. Res. Bull.*, 2015, **61**, 352–356.
39 B. Wang, M. Li, S. Zhang, H. Wu, Y. Liao and H. Li, *Appl. Catal., B*, 2023, **327**, 122454.
40 F. Xu, Z. Li, L. L. Zhang, S. Liu, H. Li, Y. Liao and S. Yang, *Green Chem.*, 2023, **25**, 3297–3305.
41 K. Van Aken, L. Strekowski and L. Patiny, *Beilstein J. Org. Chem.*, 2006, **2**, 1–7.
42 F. Wang, Z. Deng, Y. Wang, F. Yuan, X. Zhang, G. P. Lu, N. Fu and Y. Lin, *Tetrahedron*, 2022, **123**, 132985.
43 B. K. Slinker, *J. Mol. Cell. Cardiol.*, 1998, **30**, 723–731.
44 M. Boronat, A. Corma, M. Renz and P. M. Viruela, *Chem. – Eur. J.*, 2006, **12**, 7067–7077.
45 A. A. Ádám, S. Ziegenheim, Á. Papp, M. Szabados, Z. Kónya, Á. Kukovecz and G. Varga, *ChemCatChem*, 2022, **14**, 1–8.
46 R. Poreddy, C. Engelbrekt and A. Riisager, *Catal. Sci. Technol.*, 2015, **5**, 2467–2477.
47 C. Pischetola, A. Ruiz-Ruiz and F. Cárdenas-Lizana, *Chem. Eng. J.*, 2021, **418**, 129306.
48 D. R. Fandrick, D. Reinhardt, J. N. Desrosiers, S. Sanyal, K. R. Fandrick, S. Ma, N. Grinberg, H. Lee, J. J. Song and C. H. Senanayake, *Org. Lett.*, 2014, **16**, 2834–2837.
49 T. Oishi, L. I. Lugo-Fuentes, Y. Jing, J. O. C. Jimenez-Halla, J. Barroso-Flores, M. Nakamoto, Y. Yamamoto, N. Tsunoji and R. Shang, *Chem. Sci.*, 2021, **12**, 15603–15608.
50 C. J. Evoniuk, G. D. P. Gomes, S. P. Hill, S. Fujita, K. Hanson and I. V. Alabugin, *J. Am. Chem. Soc.*, 2017, **139**, 16210–16221.